博士論文番号：9971025
(Doctoral student number: 1281203)

Stepwise Patterning of Erk Activity During Somitogenesis in Zebrafish

Dini Wahyu Kartika Sari

Nara Institute of Science and Technology

Graduate School of Biological Sciences

(Submitted on 2018/02/26)

Graduate School of Biological Sciences Doctoral Thesis Abstract

Lab name （Supervisor）	Gene Regulation Research (Prof. Yasumasa Bessho)		
Name (surname) (given name)	Dini Wahyu Kartika Sari	Date	(2018/02/26)
Title	Stepwise patterning of Erk activity during somitogenesis in zebrafish. (ゼブラフィッシュ胚体節形成におけるErk活性の段階的変化の解析)		

Somites are embryonic segments, epithelial blocks of mesoderm, giving rise to the vertebrae and skeletal muscles. Somites are generated periodically by segmentation of the presomitic mesoderm (PSM). In case of zebrafish, periodicity of the segmentation is constant (around 30 min).

Periodic segmentations of somites are regulated by the clock and wavefront. The clock determines the timing of segmentation and the wavefront determines where the somite boundaries form. Notch-related factors (*Hes7* and *Lunatic fringe (Lfng)* in mouse; *her1*/*her7* and *deltaC* in zebrafish) oscillate in the PSM and serve as the clock which determines the timing of segmentation.

The wavefront was proposed to a gradient of FGF that regresses during tail elongation. The expression of FGF genes (*Fgf8* in mouse; *fgf8a* in zebrafish) is abundant in the posterior end of the PSM and declines gradually toward anterior. Manipulation of FGF gradients in PSM cells shifts the position of somite boundaries and generates somites with different size.

However, the resultant somite displays stepwise movement. It means that the temporal information of the somite segmentation clock is integrated to the spatial information of the *fgf8a* gradient in the certain step between them.

Our previous study investigated Erk activity, the downstream of FGF signaling, in fixed zebrafish embryos by using anti-phosphorylated Erk (pErk) antibody. It discovered that FGF8 gradient is converted into sharp boundary of pErk and Erk activity boundary in the

PSM moves stepwisely toward the posterior alongside with tail elongation during somite segmentation. However, since this interpretation comes from the static data, spatial and temporal resolutions are very low. To fully understand the mechanism of pre-pattern formation in the uniform PSM, it was important to observe the dynamics of Erk activity boundary in a living embryo. Therefore, in this study, I tried to develop the system of live imaging of Erk activity dynamics during zebrafish somitogenesis.

To visualize Erk activity within living zebrafish embryos, I employed a Förster (or Fluorescence) resonance energy transfer (FRET)-based Erk activity sensor called Ekarev-NLS. By using this system, high ratio of FRET/CFP could be seen in the PSM, newly formed somites, telencephalon, midbrain/hindbrain boundary as reported in the previous literatures. Inhibition of FGFR and MEK, an upstream of Erk, reduced the signal intensity of FRET/CFP. These results indicated that Ekarev-NLS FRET probe could monitor FGF/Erk signal activity in zebrafish living embryos.

To monitor the dynamic of Erk activity within PSM, I performed FRET live imaging in the PSM region of zebrafish embryos. In agreement with the notion from our static analysis, we observed that Erk stepwisely shifted stepwisely with a constant distance and timing toward the posterior end in wild type embryos. Furthermore, we revealed that in clock-deficient embryos (*her1* and *her7* double knock-down), stepwise regression of Erk activity still occurred, but the stepsize and period became irregular. In addition, cell tracing and length measurement analyses revealed that cells did not arrange around the future somite boundary within the PSM, and Erk activity border acts as a future somite boundary within the PSM in both wild type and clock-deficient embryos. My results therefore suggest that self-organization of cells occurs within the PSM and size of cell assembly is originated from the stepsize of Erk stepwise regression. Over 20 years after discovery of the first molecular signature of somite segmentation, here I provide an evidence that Erk stepwise regression with a regular timing and distance is required for cyclic formation of normal sized somites. Therefore, my live-imaging system succeeded to visualize Erk activity in living zebrafish embryos and revealed a novel spatiotemporal regulation of Erk in the PSM required for proper formation of somites in zebrafish.

List of contents

List of movies

I. Introduction

Vertebrae have a segmented structure along the body axis. However, there is no segmented structure in the earliest developmental stage so that every position is equal and uniform. In a certain timing, an embryo gets a pre-pattern, specific points are determined as a segmentation position and the uniformity is broken. In the later stage, the segment is generated from the pre-pattern, and each segment gets its character. My study focused on the earliest developmental step, where pre-pattern is formed to break the uniformity.

I. 1. Somites

Somites are embryonic segments (epithelial blocks of tissue) that differentiate into sclerotome (precursors of axial skeleton) and dermomyotome (precursors of the dorsal dermis and skeletal muscle) (Fig. 1) (Brent and Tabin, 2002).

Somite formation (somitogenesis) is believed that this process can be divided into three main stages. First, specification, the PSM is generated from the derivative of the epiblast that progressively added to the tip of tailbud of the embryo. Second, somite segmentation, epithelial blocks of cells called somites are raised from the PSM. Third, differentiation, somites are subdivided into the ventral sclerotome and the dorsal dermomyotome. And then, somite derivatives obtain anatomical identity mainly by Hox genes depending on their anteroposterior (AP) axis position (Dequeant and Pourquie, 2008).

Somite form periodically from the PSM in a different time period between species, ranging from 25-30 minutes in zebrafish embryos, 90 minutes in chicken and 120 minutes in mouse, to approximately 4–5 hours in humans (Dequeant and Pourquie, 2008; Hubaud and Pourquie, 2014).

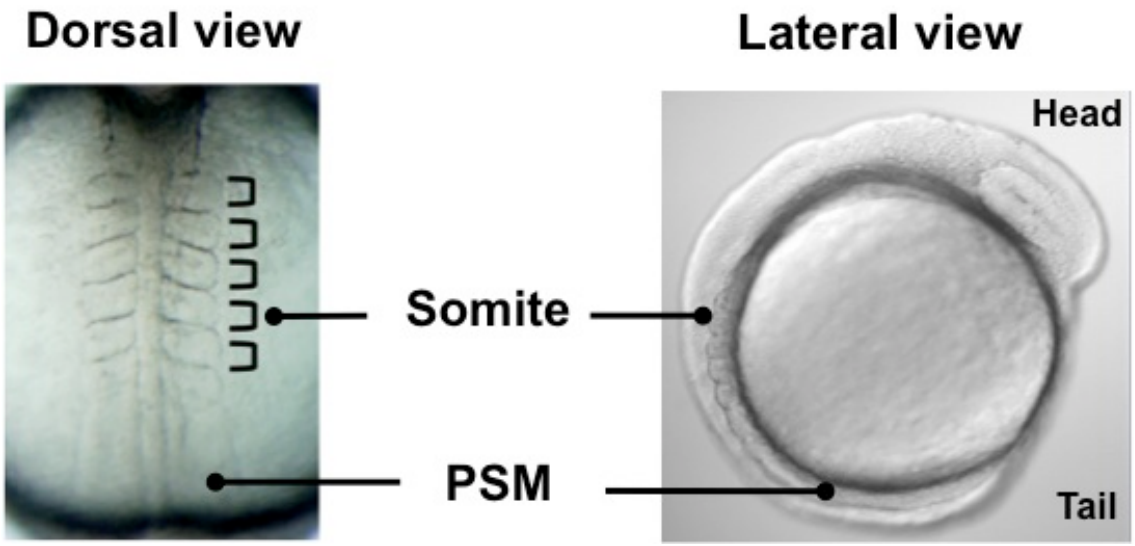

Figure 1. Dorsal and lateral view of zebrafish somites.

I.2. The clock and wavefront model

Periodic somite segmentation in vertebrate embryos is controlled by a molecular oscillator, the segmentation clock, which had been predicted as the clock and wavefront model (Cooke and Zeeman, 1976).

The clock and wavefront model proposed that PSM cells are subjected to a rapid change in cellular properties to form somite. The clock is a smooth cellular oscillator which interacts with the wavefront (a front of rapid cell change moving slowly down the long axis of the embryo) to set the time in each cell at which it will undergo a *catastrophe*, cells enter phase of rapid change in locomotory and adhesive properties when they form somites (Cooke and Zeeman, 1976). This model implies that the length travelled by the wavefront during one period of oscillation is fixed with the size of a newest segment (Hubaud and Pourquie, 2014).

Molecular evidence of the segmentation clock and a wavefront of maturation has provided over 20 years ago, although the details of the original model have not been validated (Hubaud and Pourquie, 2014).

I. 3. The segmentation Clock

The first molecular sign of the existence of an oscillator (the segmentation clock) was come up by the periodic expression of the mRNA encoding hairy and enhancer of split 1/*c-hairy1* (the transcription factor HES1) in the chicken embryo PSM (Palmeirim et al., 1997). They showed that *c-hairy1* mRNA is expressed in a highly dynamic manner appearing as a caudo-rostral wave, which is repeated during the formation of every somite.

The dynamic expression of *c-hairy1* is not a result of cell movements neither to the periodic production of a secreted diffusing signal, but is an autonomous oscillation in gene expression that synchronized among the neighboring PSM cells (Palmeirim et al., 1997).

Later on, other cyclic genes were reported in chicken (*lFng*, *c-hairy2,* and *c-hey2*) (Jouve et al., 2000; Leimeister et al., 2000; McGrew et al., 1998); mouse (*Lfng, Hes1, Hes5, Hes7,* and *Hey1*) (Bessho et al., 2001a; Bessho et al., 2001b; Bessho et al., 2003; Dunwoodie et al., 2002; Forsberg et al., 1998; Hirata et al., 2002); and zebrafish (*deltaC, her1*, and *her7*) (Henry et al., 2002; Holley et al., 2002; Jiang et al., 2000; Oates and Ho, 2002). In all the species studied, only hairy-related genes seem to display cyclic expression among various species, suggesting that this class of transcription factors is the core of the vertebrate clock (Bessho and Kageyama, 2003; Hubaud and Pourquie, 2014). In chicken, mice, and zebrafish, the cyclic genes are mostly involved in Notch, Wnt and FGF signaling pathways (Dequeant et al., 2006; Goldbeter and Pourquie, 2008; Krol et al., 2011).

I.4. The wavefront

The wavefront was proposed to a gradient of FGF (Dubrulle et al., 2001; Sawada et al., 2001) and Wnt signaling (Aulehla et al., 2003) that regresses alongside with axis elongation. If the expression levels of FGF and Wnt are manipulated, the position of somite boundary will be shifted and somite size will become different (refs).

fgf8 messenger RNA is transcribed just in the posterior tip of the embryo, and degraded progressively, producing in the gradient of the mRNA in the posterior part of the embryo (Dubrulle and Pourquie, 2004). Furthermore, Delfini et al. reported that ERK (the effector of the FGF gradient) controls the motility of PSM cells (Delfini et al., 2005), suggesting that the mesenchymal PSM cells allows to undergo proper segmentation because cell movement along the PSM is limited. At a particular threshold of FGF and Wnt signaling (the determination front), cells of the PSM become competent in response to the segmentation clock (Dubrulle et al., 2001).

I.5. The segmentation program (from oscillations to segments)

Mesoderm posterior (MESP) family members are activated simultaneously by the competent PSM cells (Saga, 2012). MESP genes (*Mesp1* and *Mesp2* in mice; *c-meso1* and *c-meso2* in chickens; and *mespa* and *mespb* in zebrafish) are the first sign of the future segment boundary. Inactivation MESP genes in the PSM blocks segment formation (Buchberger et al., 1998; Buchberger et al., 2002; Saga et al., 1997; Sawada et al., 2000).

In zebrafish, *fgf8a* gradient is converted into sharp boundary of pErk domain that is located more posteriorly than the *mespb* stripe. Furthermore, Erk activity boundary in the PSM moves stepwisely during tail elongation and the anterior limit of Erk activity represents the future somite boundary. Moreover, somite segmentation clock controls the regularity of stepwise movement of the Erk activity boundary (Akiyama et al., 2014). Dusp6 inhibitor treatment to manipulate FGF/Erk pathway alters the phosphorylated ERK domain anteriorly and induce the formation of a smaller somite after four normal somites are generated. This study proposed that a future somite boundary is located at the posterior PSM before *mespb* activation (Akiyama et al., 2014).

This concept is consistent with heat-shock treatments in zebrafish embryos that

revealed the possibility of future segment boundary exist more posterior region, before *mespb* activation within PSM. In these experiments, brief heat shock treatment was not affect somite formation at the same time of treatment but rather, on average, the fifth somite (after 4 somites form normally) (Roy et al., 1999).

I.6. Thesis preview

However, since these interpretations come from the data using fixed embryos, I do not know yet whether Erk activity boundary represents as a future somite boundary and stepwisely shifts within the uniform PSM in living zebrafish embryos.

In this study, I used Ekarev-NLS and succeeded to visualize Erk activity within living embryos. Within the PSM, Erk is activated in the posterior part of the PSM and generated with a sharp boundary. Time-lapse analysis revealed that the Erk boundary within the PSM shifts stepwisely along with the somite segmentation cycles. Cell tracing experiments confirmed that the Erk activity boundary will become a real somite boundary. Furthermore, I observed Erk activity dynamics in embryos without the clock and found a novel role of FGF/Erk activity boundary within the PSM.

II. Materials and methods

II.1. Zebrafish

Wild-type zebrafish embryos in this study were maintained under laboratory conditions and staged according to standard protocol (Kimmel et al., 1995). The embryos for the experiments were obtained by natural mating, which was conducted by using 4 to 6 set of matting box, each contain of 2 male and 2 female, respectively. The fishes were set at 07:00 – 09:00 p.m. of one day before the mating, which were conducted at around 09:30 11:00 a.m. Male and female fish were put together during the mating process and embryos were collected 5 minutes after mating (fertilization) for the probe injection.

II.2. Morpholinos (MOs)

The following antisense MO oligonucleotides against *her1 and her7* were obtained from Gene Tools: *her1*-MO: 5′ TTCGACTTGCCATTTTTGGAGTAAC-3′ and *her7*-MO: 5′ -CAGTCTGTGCCAGGATTTTCATTGC-3′ (Henry et al., 2002).

II.3. Synthesis of mRNA encoding the Erk biosensor Ekarev-NLS

The Erk biosensor termed Ekarev-NLS comprises an enhanced cyan-emitting mutant of GFP (ECFP), a WW domain, an EV linker, an Erk substrate, a yellow fluorescent protein for energy transfer (Ypet), and a nuclear localization signal (NLS) (Komatsu et al., 2011). When Erk phosphorylates the Erk substrate, the WW domain binds to the Erk substrate, thereby bringing ECFP closer to Ypet and inducing FRET from ECFP to Ypet. The pCS2-*Ekarev-NLS* subcloned from pPBbsr2-3594NLS (Komatsu et al., 2011) was used as a template for mRNA synthesis. *Ekarev-NLS* mRNAs were synthesized using the SP6 mMessage mMachine system (Thermo Fisher Scientific).

II. 4. Injection of mRNA/MO into zebrafish embryos

Ekarev-NLS mRNAs 100 pg were injected into the yolk of one-cell-stage zebrafish embryos under stereomicroscope by using FemtoJet microinjector (Eppendorf) as described previously (Matsui et al., 2011). When I disrupted zebrafih segmentation clock, *Ekarev-NLS* mRNAs (100 pg), *her1*-MO (6.25 ng), and *her7*-MO (6.25 ng) were co-injected. Injected embryos were used for time-lapse imaging.

II.5. Time-lapse imaging

Zebrafish embryos expressing Ekarev-NLS at 12-13 hpf were dechorionated and embedded in 1% low melting agarose, which be positioned at the center of a glass-bottom dish. The embryos were carefully oriented and fixed in a dorsal or lateral position. When the desired position is fixed, the glass bottom disk than filled with fish medium.

Dorsal view imaging was performed with 20x objective lens magnification. Compared with lateral view, dorsal view has higher resolution image, but cells tracking analysis from the Erk activity boundary to the corresponding real somite could not perform because only can take a time-lapse imaging in a short time (less than 2 hours). To solve this problem, time-lapse image of Erk activity within somite and PSM region from lateral was taken with 10x objective lens magnification and 1.5 zoom.

Fluorescence spectra were acquired by using a LSM710 confocal microscope (Zeiss) in the lambda scanning mode upon excitation of CFP at a wavelength of 440 nm. Auto exposure in the configuration window was used to set up the laser power, pinhole, master gain, digital offset, and digital gain. T-PMT button was also clicked to obtain both a fluorescence and a bright-field data. Z-stack was set to get several layers of the pictures. “Set First” button was clicked in the desired starting point and then “Set Last” button was clicked in the desired ending point. After stopping the scan, optimal interval layer was chosen. For

every single take, the depth of picture was set up 8 to 10 Z layer or stack, with 5-10 mm spacing of each stack. “Range Indicator” was used to optimize laser power, pinhole, master gain, digital offset, and digital gain of the sample. If saturated pixels (red) and zero value (blue) were observed, Split View was used to optimize each channel by changing master gain, digital offset, and digital gain. To obtain high resolution data, 512 x 512 frame size, slow scan speed (7), and four times averaging in the Acquisition Mode window were used. “Time Series” was set to obtain pictures every 5 minutes for 3 hours under temperature 28.5°C. Last, the CFP and YFP signal from the time-lapse images were separated using “Linear unmixing” mode according to the CFP and YFP signal references.

II.6. Image analysis

Pictures were selected by Zen software and proceed by MetaMorph software (Universal Imaging, West Chester, PA). FRET/CFP ratio images were made after background subtraction and the intensity was indicated by colors from red (high) to blue (low) (Komatsu et al., 2011). After FRET/CFP ratio images were created, median filter, non linear filtering technique but still preserve the edges while reducing the noise, 15px x 15px was applied to reduce the signal noise.

II.7. Determination of the anterior limit of Erk signal within PSM

A line along the entire PSM region of ratio image time-lapse images was drawn to generate a kymograph (graphical representation of spatial position over time in which a spatial axis represents time). For the quantification, the FRET and CFP intensities from the kymograph were exported to Excel software (Microsoft Corporation, Redmond, WA). Graph of the data set were made using Microsoft Excel.

The anterior limit of the Erk activity boundary was determined by combining all information from visual observation, kymograph, and signal intensity (when the signal goes up significantly).

II. 8. Cell tracking

Cell tracking was performed using FIJI (ImageJ), from the cells around future somite boundary and somite segment region.

II.9. Immunohistochemistry

Immunohistochemistry were performed as described previously (Matsui et al., 2005; Matsui et al., 2011). Embryos were fixed with 4% PFA at 4 ºC for 10-16 h and dehydrated with methanol. Re-hydrated embryos were treated with 1% Triton X-100, 6% H2O2 in PBS for 20 min, washed with MABDT (0.1 M maleic acid pH 7.5, 150 mM NaCl, 1% DMSO, 0.1% Triton X-100), and blocked with 2% FBS in MABDT for at least 1 h. The embryos were then incubated with mouse monoclonal antibodies against dp-Erk (1:2000; Sigma) in MABDT at 4 ºC for at least 24 h. To detect phosphorylated Erk, the embryos were washed with MABDT and incubated with HRP goat anti-mouse IgG (1:100; Invitrogen) or Alexa Fluor 555 goat anti-mouse IgG (1:250; Invitrogen) at 4 ºC for at least 12 h. After MABDT washing, the signals were detected and amplified using an Alexa Fluor 488-Tyramide Signal Amplification Kit following the manufacturer's instructions (Invitrogen). Immunofluorescence signals were visualized and photographed using LSM 700 or LSM710 confocal microscope (Zeiss).

II.10. SU5402 (FGFR inhibitor) and PD184352 (MEK inhibitor) treatment

Zebrafish embryos expressing *Ekarev-NLS* at 12-13 hpf were dechorionated and embedded in 1% low melting agarose. Time-lapse image acquisition was performed with a LSM710 confocal microscope (Zeiss) for 15 minutes and then treated with 0.2 mg/ml SU5402 or 1.5 μM PD184352, and continued time-lapse imaging again for 1 hour. Pictures were obtained every 5 minutes as described before.

II.11. Statistical analysis

Statistical comparisons were analyzed by two-tailed Students's *t*-test. Results in the *t*-test were considered significant when $P<0.05$.

III. Results

III.1. Sensitivity and specificity of FRET biosensor Ekarev-NLS to monitor Erk activity in zebrafish embryos

Our previous study reported that *fgf8* gradient is converted into sharp boundary of Erk activity within the PSM (Akiyama et al., 2014). Moreover, this sharp boundary of Erk activity moves stepwisely toward posterior along with the tail elongation, and the anterior limit of Erk activity boundary represents the future somite boundary. However, since these interpretations come from the data using fixed embryos, I do not know yet the dynamic of Erk activity. In addition, it remains unclear whether Erk activity boundary stepwisely shifts within the uniform PSM, and whether the boundary represent as a future somite boundary in living zebrafish embryos. To visualize Erk activity within living zebrafish embryos, I employed a Förster (or Fluorescence) resonance energy transfer (FRET)-based Erk activity sensor called Ekarev-NLS (Fig 2).

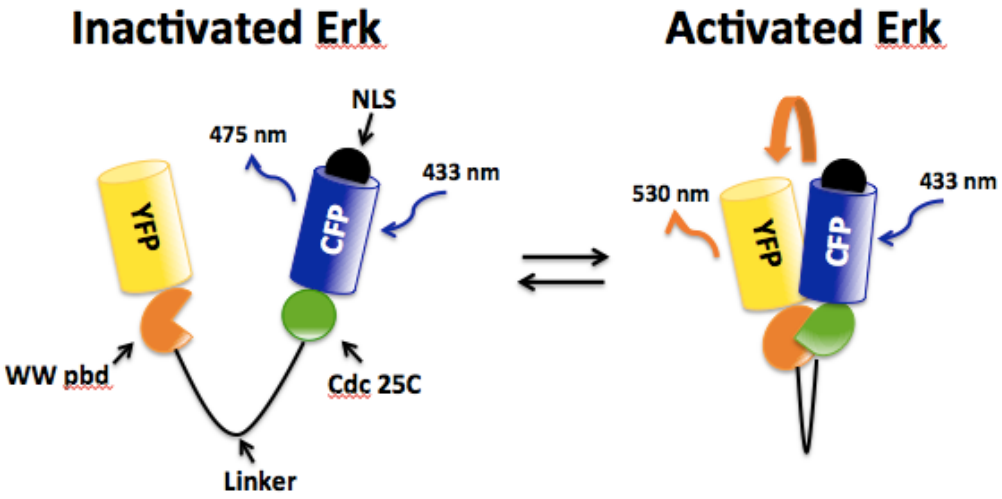

Figure 2. Ekarev-NLS activation model. Ekarev-NLS consist of donor: ECFP, acceptor: Ypet, EV linker: 116-244 aa, sensor domain: Cdc25C (containing consensus MAPK target sequence (PRTP)), ligand domain: WW phosphor-binding domain, and NLS: Nuclear Localization Sequence (Komatsu et al., 2011). A donor chromophore (CFP), initially in its electronic excited state, may transfer energy to an acceptor (YFP). Once activated, Erk will phosphorylate their target such as Cdc25C. Next, WW phospho-binding domain will bind to this phosphate complex, and then CFP and YFP become close. Finally signal from CFP will transfer to YFP and FRET will come up.

Injection of *Ekarev–NLS* mRNA was performed just after fertilization. After the embryo reached 8 somite stage, time-lapse imaging was carried out and ratio of FRET/CFP was calculated. Injection of *Ekarev-NLS* mRNA in zebrafish embryos delivered this probe in all cells within embryos, but high FRET signals were observed just in the midbrain-hindbrain boundary, newest somite and the PSM (Fig. 3B).

In somites, FRET signals can be seen in the older somite (SII), newly formed somite (SI), and forming somite (S0), which has not yet detached from the PSM. The highest FRET signal was found in SI (Figure 3C). Low FRET signal also could be observed in PSM S-II (Fig. 3C). The pattern of FRET signals closely resembles the activated domains of Erk (p-Erk) (Fig. 3A) and the expression domains of *fgf8* as shown previously (Sawada et al., 2001; Stolte et al., 2002). Based on these similarities, I thought that Ekarev-NLS may be able to monitor Erk activity in zebrafish.

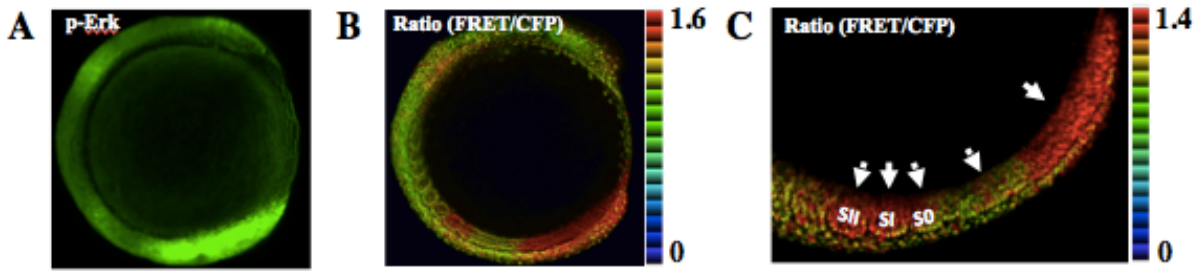

Figure 3. Ekarev-NLS signal in zebrafish embryo. (A) p-Erk immunostaining, (B) C) ratio image of FRET/CFP in zebrafish embryos. Arrows indicate spatiotemporal of Ekarev-NLS signal in somite and PSM. Red color means highest signal and blue color means lowest signal.

To test this possibility, a FGF signal cascade was inhibited using FGFR inhibitor SU5402 (Fig. 4A) (Mohammadi et al., 1997; Sawada et al., 2001).

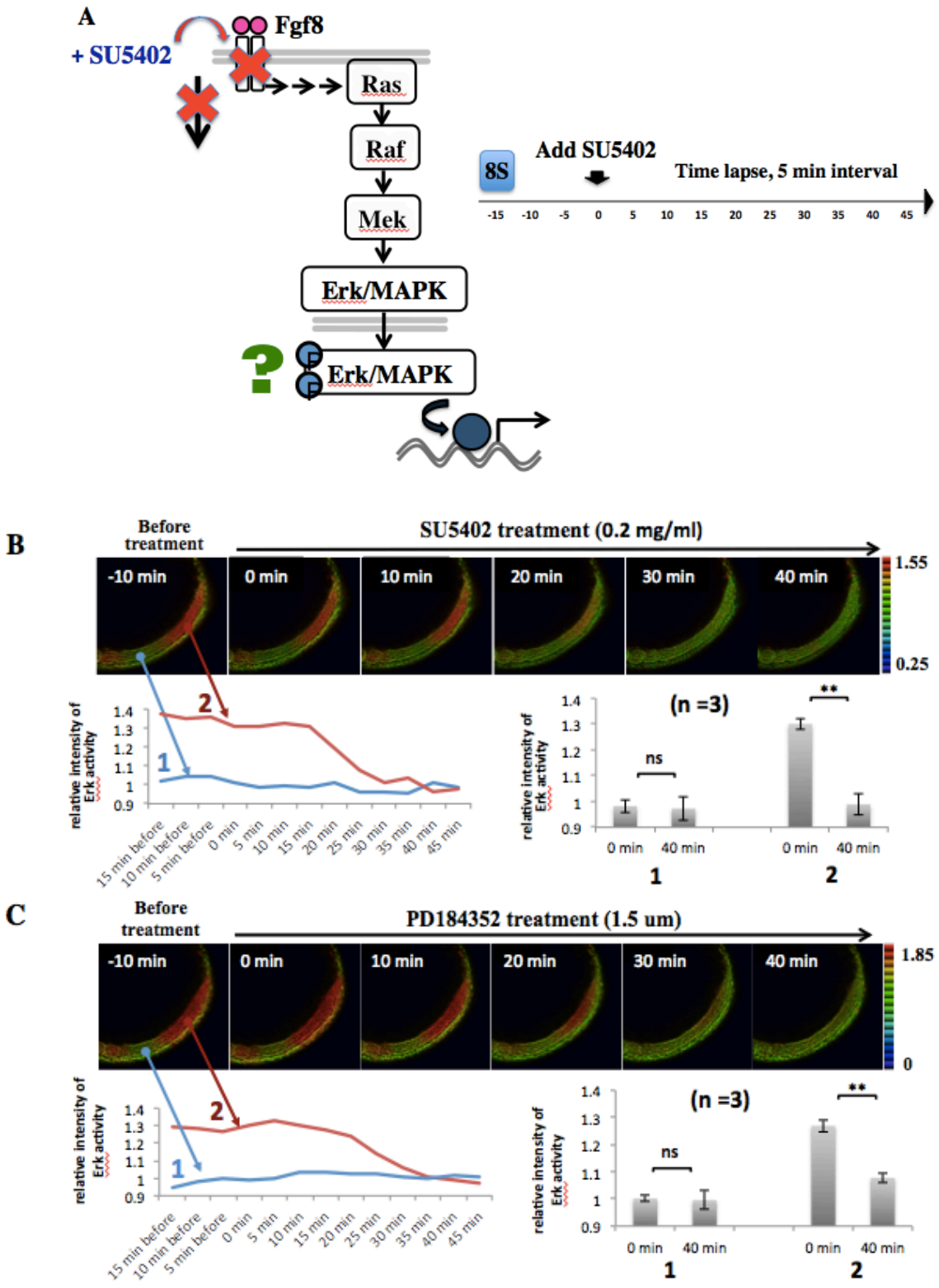

Figure 4. FGF signal inhibition reduces FRET signals which detected by Ekarev–NLS probe. (A) Schematic of the experimental design, Time-lapse imaging was performed using confocal microscope for 15 minutes, then treated with 0.2 mg/ml SU5402 and continued time-lapse imaging for 1 hour. Pictures were obtained every 5 minutes. (B) FGFR inhibitor (SU5402) treatment, (C) MEK inhibitor (PD184352) treatment. Data are represented as means + SE. *p < 0.05, Student's *t*-test; n = 3.

SU5402 (0.2 mg/ml) was applied to the embryo at the 8-somite stage under confocal microscope and then time-lapse images were taken (Fig. 4A and Movie 1). Before treatment (Fig. 4B and Movie 1), in low FRET signal region as shown in blue line, the FRET signals did not change during time-lapse imaging; but in high FRET signal (red line), FRET signals went down gradually after SU5402 treatment, and most of the signals were gone after 30 minute. I also observed that significant difference of the FRET signals before and after treatment (Fig. 4B). These results clearly show that FGFR inhibitor can inhibit the FRET signals.

We also used PD184352 (1.5 μM), which can inhibit MEK, an upstream of Erk and downstream of FGFR (Sebolt-Leopold et al., 1999). As expected, PD184352 could inhibit the FRET signals (Fig. 4C and Movie 2). These results indicate that Ekarev-NLS FRET probe can monitor FGF/Erk signal activity in zebrafish living embryos.

III.2. The Erk activity boundary moves stepwisely in zebrafish living embryos PSM

To investigate dynamics of Erk activity within the PSM of zebrafish living embryos, I performed time-lapse imaging at higher magnification (Movie 3). Because high and low FRET signals could be seen at the posterior and anterior PSM, respectively, an ON/OFF boundary of Erk activity was observed when the time-lapse imaging is started. Along with the time progression, the boundary was shifted to posterior. To understand how the boundary shifts along with somite segmentation, I generated kymograph (Fig. 5B) and investigated the tempo and width of the shifts.

Boundary of Erk activity within the PSM in wild-type zebrafish embryos was observed at B-4 position, and the stepwise shift about one somite length toward posterior in a regular time (~30 min) as somite segmentation period (Fig. 6B and 5C). I did same analyses by using several samples and could obtained data showing that the periodicity of

both somite segmentation and stepwise shift of Erk activity boundary occurred constantly (a period of 25-30 minutes) (Fig. 5D).

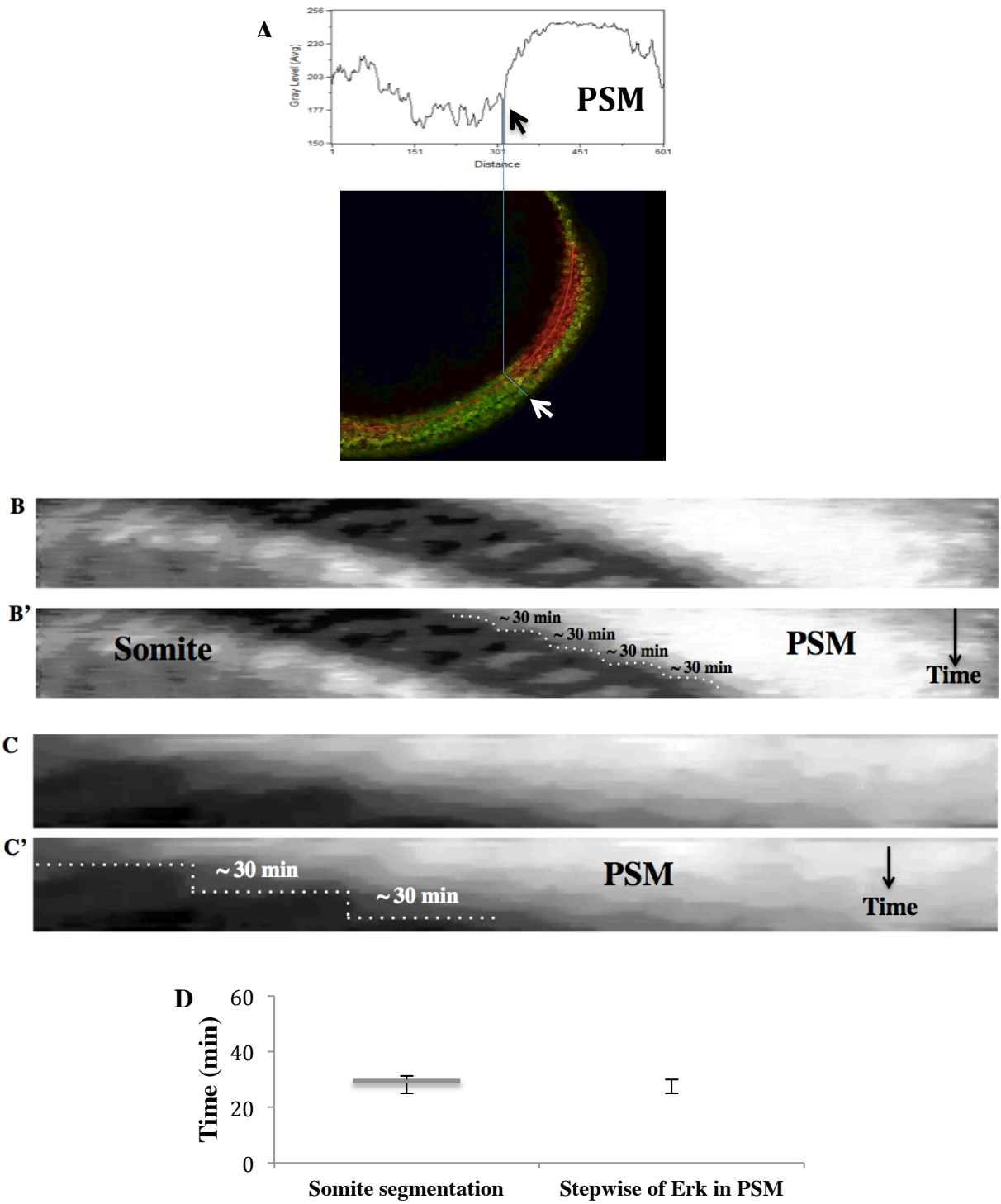

Figure 5. The Erk activity boundary moves stepwisely in zebrafish living embryos PSM. (A) Determination of the anterior limit of Erk signal within PSM (lateral view), a line along the entire PSM region of ratio image time-lapse images was drawn (line-scan) to generate a graph and kymograph. The signal intensity (upper panel) and visual observation (lower panel) were compared to estimate the position of the anterior boundary of Erk in PSM. Anterior boundary of Erk was

estimated when the signal goes up significantly (arrow). (B and C) Kymograph generated from time-lapse images, (B) lateral view, (C) dorsal view, left to right means anterior (somite region) to posterior (PSM region), up to bottom (black arrow) means time progression, discrete pattern of Erk activities are shown in dash line. (D) Box and whisker plot of somite segmentation and stepwise of Erk activity in PSM timing, (n=20).

III.3. The Erk activity boundary within the PSM will be the real somite boundary

If Erk boundary acts as the future somite boundary, Erk boundary cell will become the real somite boundary cell. To test this, the cells around the boundary were tracked.

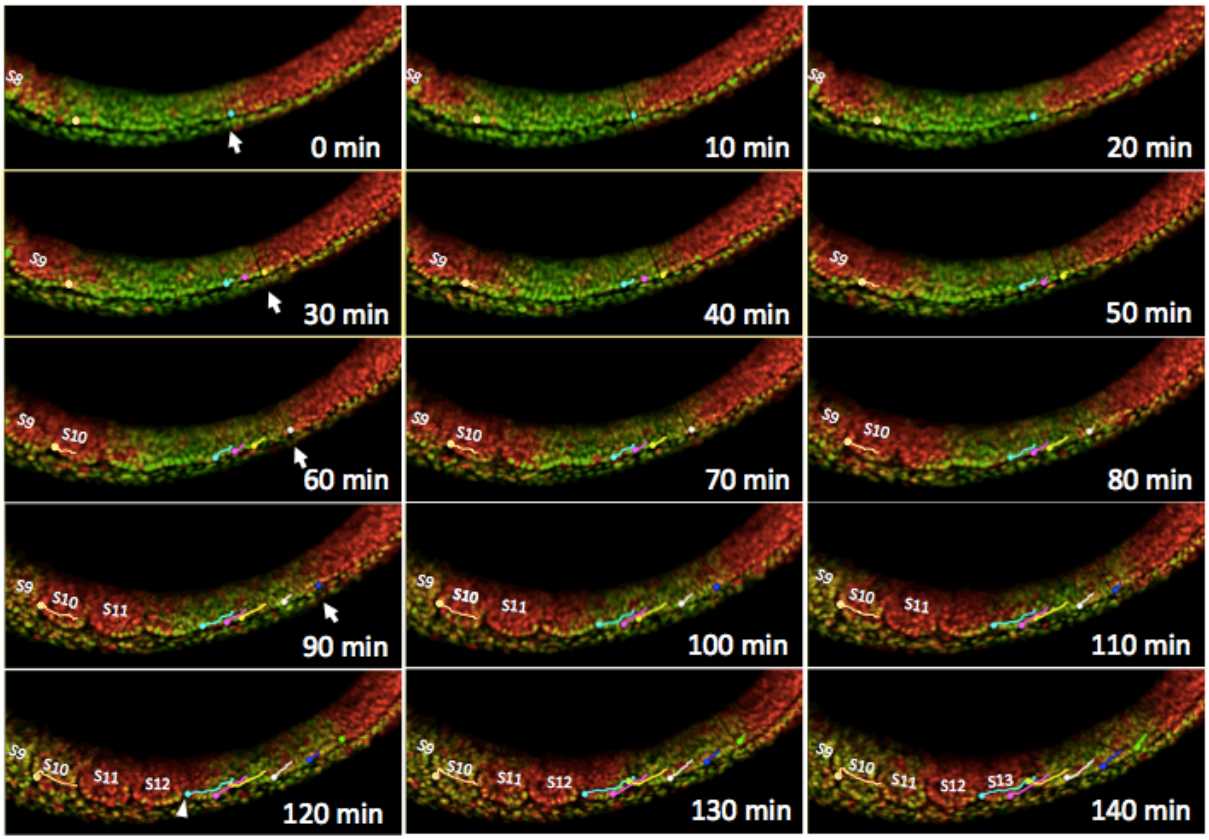

Figure 6. Cell tracking in WT. Light blue, yellow, dark blue, and yellow are cells in the Erk activity boundary (arrow) will become the real somite boundary cell (white arrow head); pink cell does not located in the Erk activity boundary will not become the real somite boundary. Stepwise pattern of Erk activity occurs regularly every 30 minutes.

Tracking the cells from the anterior border of Erk activity in PSM region show that these cells (every cell in anterior boundary of Erk in PSM, see Fig. 6, white arrow) will become the anterior boundary of a real somite (Fig. 6, white arrowhead). Tracking the cells which do not locate the anterior border of Erk activity in PSM region show that these cells

will not become the anterior boundary of somite (Fig. 6, pink cell). Anterior boundary of Erk activity in PSM shift posteriorly after certain time point, when the Erk signal of a group of cells (about one somite length) suddenly OFF. Both somite segmentation and Erk stepwise movement constantly occurs every about 30 minutes (Fig 6). These data indicate that Erk activity boundary move stepwisely and constantly in zebrafish living embryos, and that the Erk activity boundary within the PSM corresponds to the real somite boundary.

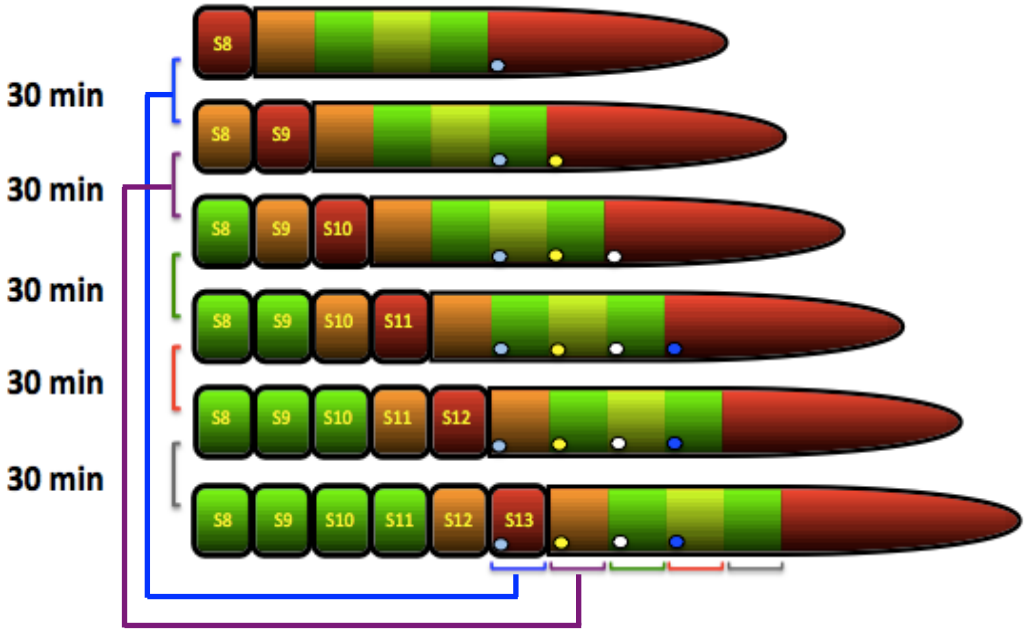

Figure 7. A model of stepwise pattern of Erk activity boundary in WT. Time indicate stepwise movement of Erk activity within PSM (red colour in the PSM region). Erk activity boundary move stepwisely and constantly in zebrafish living embryos. Cell arrangement did not change around the future somite boundary within the PSM and cell of Erk activity boundary will become a real somite boundary cell.

III.4. Double knockdown of *her1* and *her7* leads to irregular stepwise regression of Erk boundary within the PSM

In somite formation, the role of the clock has been currently challenged. Dias et al. reported that, although without cyclic expression of Notch related genes, many somites form simultaneously from non-somite mesoderm treated with Noggin (Dias et al., 2014). These somites have normal shape, size, axial identity, and fate; but lack of rostral and caudal

subdivision. Thus, Dias et al., 2014 proposed that local cell-cell interaction control size and shape of self-organizing structures of somite.

However, a model only from tissue mechanics could not explain why some mutants of the segmentation clock (for example, *Hes7*-null mice or the zebrafish *her1 and her7* morphant) undergo changes in segment length. Somite segmentation occurred uncoordinatedly but somites are still irregularly arranged (Bessho et al., 2001; Henry et al., 2002).

Thus, several questions are remaining. How do irregular somites form in clock-deficient embryos? What determines the size of somites? How do the different signaling pathways interact?

To challenge these questions, I knocked down two segmentation clock genes, *her1* and *her7*, and performed time-lapse analyses to observe the dynamics of the anterior limit of Erk activity in the clock deficient embryos. In this knockdown situation, high and steep signal in the Erk activity boundary within PSM still could be seen (Fig. 8A and Movie 4), suggesting that the segmentation clock is not required for the generation of Erk activity boundary within the PSM. However, time-lapse imaging revealed that stepwise shift of Erk occurred, but the tempo became irregular (Fig. 8A and Movie 4). In addition, variations of tempo and width of the shift of the Erk activity boundary became bigger than those of wild types (Fig. 8B).

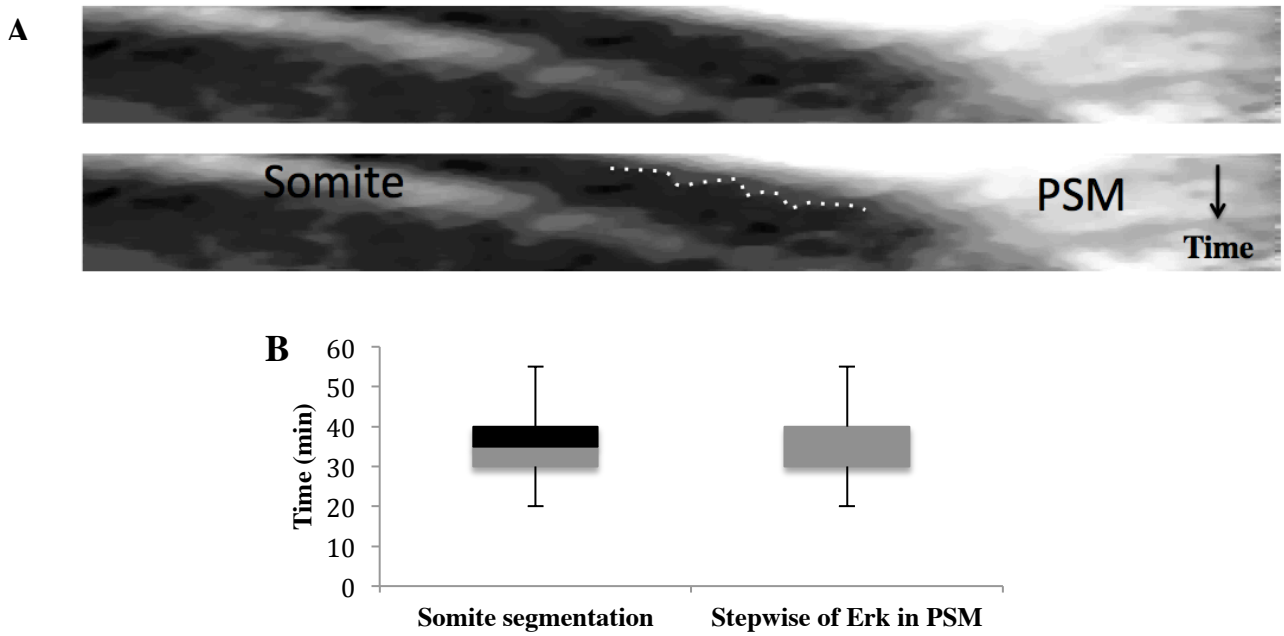

Figure 8. Stepwise pattern of Erk activity boundary within PSM moves irregularly in *her1* and *her7* KD. (A) Kymograph generated from lateral view of *her1* and *her7* KD time-lapse images. Left to right means anterior (somite region) to posterior (PSM region), up to bottom (black arrow) means time progression, discrete pattern of Erk activities are shown in dash line. (B) Box and whisker plot of periods of somite segmentation (n=18) and stepwise of Erk activity in the PSM (n=18).

Although stepwise pattern of Erk activity boundary become irregular, the boundary cell located at Erk activity boundary will become the real somite boundary cell in the clock deficient embryos. For instance, every cell in anterior boundary of Erk in PSM as shown in yellow, white and blue cells (Fig. 9, arrow) still will become the anterior boundary of a real somite (Fig. 9, arrowhead). From these data, we conclude that zebrafish embryos without clock resulted in the irregularity timing of the stepwise shift of the Erk boundary during somite segmentation, leading to segmentation defects of somites (somite getting smaller or bigger).

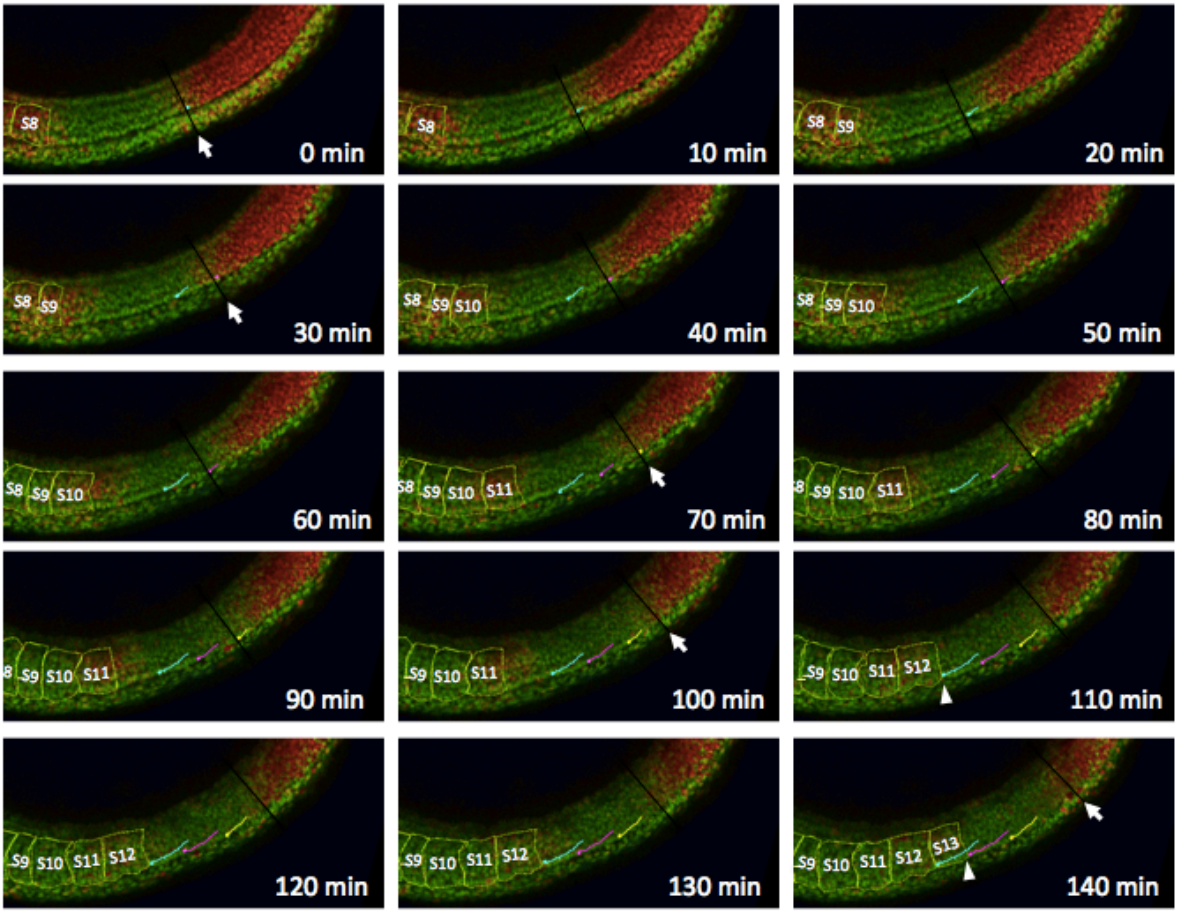

Figure 9. Cells tracking in *her1* and *her7* KD. Yellow, white, and blue are cells in the Erk activity boundary (arrow) will become the real somite boundary cell (white arrow head). Stepwise pattern of Erk activity occurs irregularly and metameric structure of somites are disrupted.

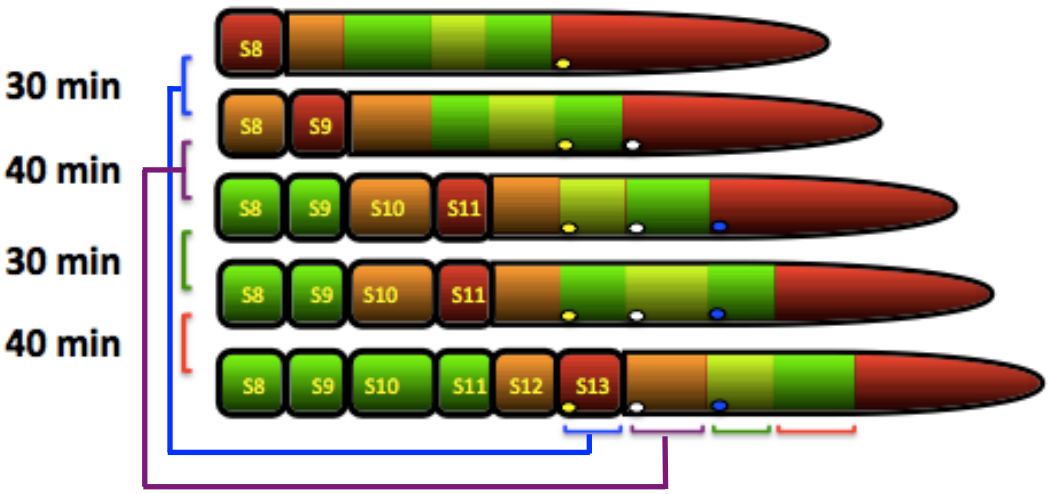

Figure 10. A model of stepwise pattern of Erk activity boundary in *her1* and *her7* KD.. Time indicate stepwise movement of Erk activity within PSM (red colour in the PSM region). Erk activity boundary move stepwisely and irregularly in KD zebrafish living embryos. Cell arrangement did not change around the future somite boundary within the PSM and stepwise timing of future somite boundary has positive correlation with the size of corresponding somites.

III.5. Irregularity timing of stepwise shift of Erk boundary in double knockdown of *her1* and *her7* correspond to the irregular somite segmentation

Erk activity boundary within the PSM moves stepwisely and every cell of the boundary becomes the real somite boundary. Is there any correlation between stepwise timing and correspond somite length? To test this possibility, I measured the period of stepwise pattern of Erk and the somite size.

In WT, stepwise of Erk activity in PSM occurred every 30 min, and this constant stepwise movement reflected to almost same size of correspond somite length (~50 μm). In WT, variations of both stepwise timing and correspond somite length were very small (Fig. 11 A).

On the other hand, when clock gene was disrupted, stepwise timing of Erk activity became irregular and correspond somite length became variable. For example, when stepwise timing occurred within 30 minutes, the correspond somite length was 50 μm; but when stepwise timing occurred within 35 minutes, the correspond somite size was 55 μm (Fig. 11B).

These data suggest that there is a positive correlation between stepwise timing and correspond somite length: shorter stepwise movement of Erk activity boundary reflects to the smaller size of corresponding somite, and longer stepwise movement reflects to the bigger corresponding somite.

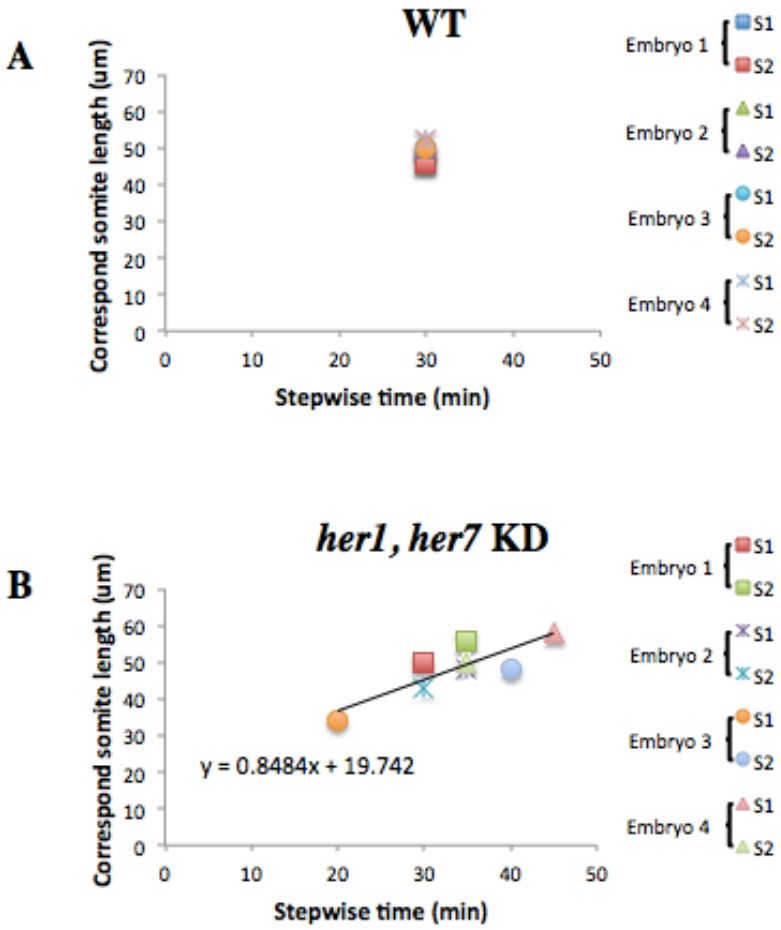

Figure 11. Correlation of stepwise timing of Erk activity within PSM and correspond somite length. (A) WT and (B) her1, her7 KD. n=8.

III.6. Stepwise pattern of Erk activity boundary contribute to the real somite segment

The dynamic behavior of future somite boundary by live-imaging of FGF/Erk activity boundary within PSM showed that both tempo and size of stepwise shift (stepsize) of future somite boundary become irregular in the PSM of *her1* and *her7* double knockdown embryos. In addition, cell tracing and length measurement analyses revealed that cell arrangement did not change around the future somite boundary within the PSM, and stepsize of future somite boundary have high correlation with the size of corresponding somites. Our results therefore suggest that self-organization of cells occurs within the PSM and the size of cell assembly is originated from the stepsize of future somite boundary (Fig. 7, Fig. 10, and Fig. 12.)

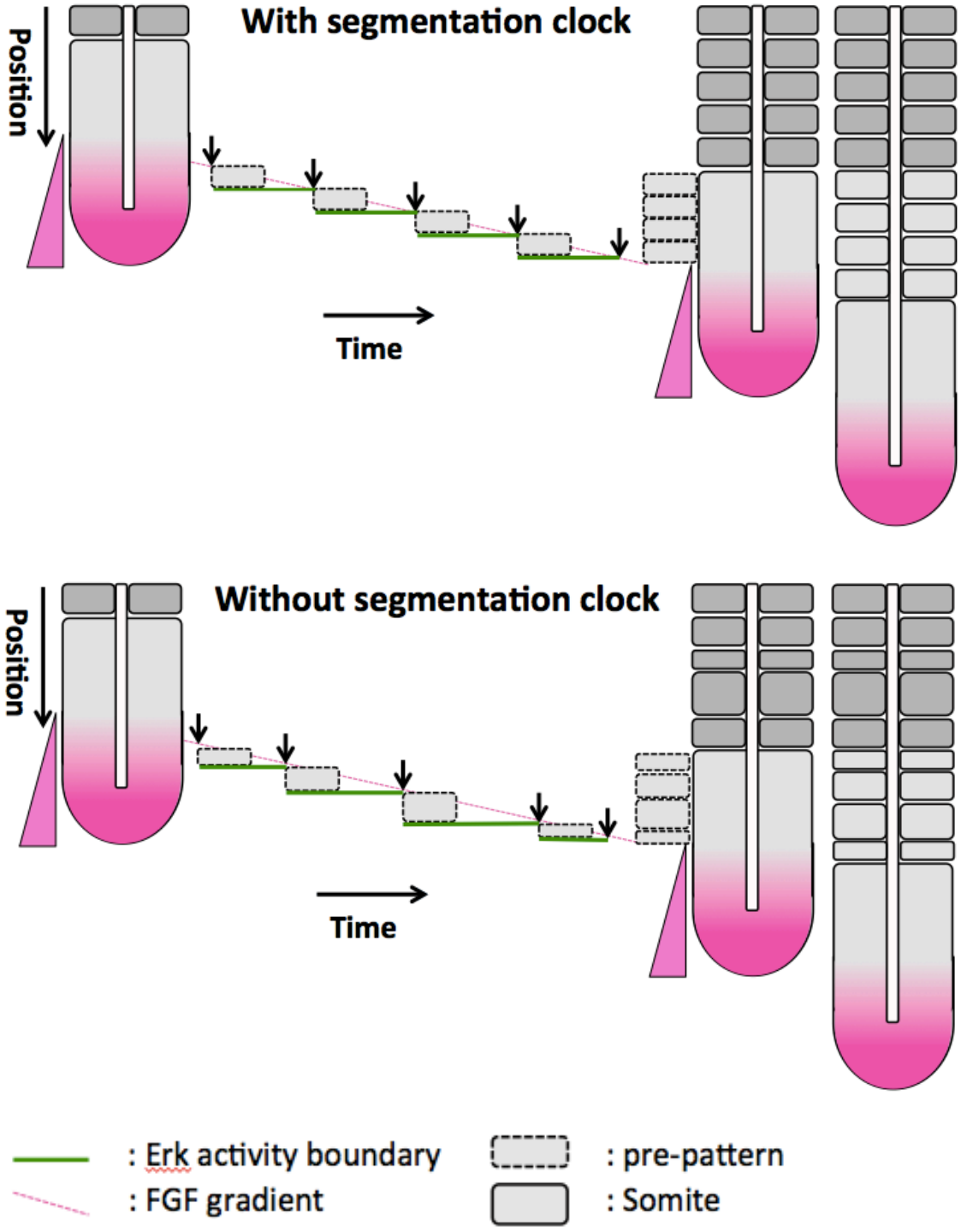

Figure 12. A conceptual model of somite segmentation. Upper panels; With segmentation clock, Erk activity boundary moves stepwisely toward posterior in a constant timing, as a result, pre-pattern formation occurs which is determine the proper positioning of the somite boundary, leading the constant size of somite. Lower panels; Without segmentation clock, Erk activity boundary still moves stepwisely in a random timing, leading the variation size of corresponding somite. Erk activity boundary meets with the wavefront (the sloping line) at irregular timing; it means that the position of future somite boundary is determined on the wavefront even in the without clock situation.

IV. Discussion

Periodic somite segmentation in vertebrate embryos is controlled by a molecular oscillator, the segmentation clock. The presence of the clock had been predicted as the clock and wavefront model (Cooke and Zeeman, 1976). Clock controls the timing of the somite segmentation and wavefront determine the position of the somite segment. In respond to clock signals, competent PSM cells simultaneously activate genes of the mesoderm posterior (MESP), the master regulators of the segmentation program, that regulates the formation of the future segment boundary (Saga, 2012). Recently, in zebrafish, it has been proposed that the existence of segmental pre-pattern occurs in the posterior PSM before *mespb* activation. By using fixed embryos, Akiyama et al. show that gradient of *fgf8* mRNA gradient is converted into periodic movement of sharp boundary of Erk activity in a stepwise pattern within the uniform PSM, and the periodic movement correlates with the somite segmentation (Akiyama et al., 2014). However, these results are obtained from fixed embryos so that there are remaining questions. For instance, how FGF/Erk activity boundary shift stepwisely? Will the FGF/Erk activity boundary cell become real somite boundary cell?

In this study, to provide clear evidence of the dynamic activity of Erk activity boundary within PSM in zebrafish living embryo, I employed FRET biosensor Ekarev-NLS. FRET signal can be seen in PSM, newest somite, and midbrain-hindbrain. This FRET signal mimics the *fgf8* expression and p-Erk domain in zebrafish embryo. Since the FRET signal can be seen in the several location as same as *fgf8* expression, this biosensor is promising probe to observe the dynamic activity of Erk in several regions of zebrafish living embryo.

Hereafter, I focused on the somite and PSM region to study the dynamic activity within PSM more deeply. Spatial temporal signal of FRET signal can be seen in newest somite (S1), also S0 and SII, but the highest FRET signal was in the SI. Later on, I used this

signal parameter to determine the newest somite boundary (B0) instead of the morphological data from bright field image as reported previously (Retnoaji et al., 2014).

From the time-lapse of FRET/CFP ratio image and cell tracking data, the boundary of Erk activity within PSM at the B-4 position. Erk activity boundaries were located on the posterior part of newest somite boundary after 4 somites length of pre-pattern somite. My estimation that the position of Erk boundary within PSM in B-4 is different from that of Akiyama et al, 2014 (the Erk boundary is located at B-4). This discrepancy may account for following reason. As I mentioned, B0 position is needed to estimate by visual observation from bright field images in fixed embryos, but this interpretation is very difficult. To estimate B0 position easily, I used FRET signals located at S1 as a marker and succeeded to find estimation of B0 position.

Erk activity boundary moves stepwisely and periodically in zebrafish living embryos as shown in the kymograph data (Fig. 5B and 5C). Moreover, cell tracking show that Erk activity boundary cells will become the real somite boundary. These evidences suggest that Erk activity boundary within the PSM correspond to the real somite segment and periodic movements of stepwise pattern of Erk activity boundary indicate that clock controls the regularity of this pattern.

From the time-lapse images, the cells seemed to move toward the posterior end. To check whether this is real movement or not, I tried to compare the cell in the somite boundary, as a standard (which should be undergo minimal movement), and cells in the PSM region (Fig. 13).

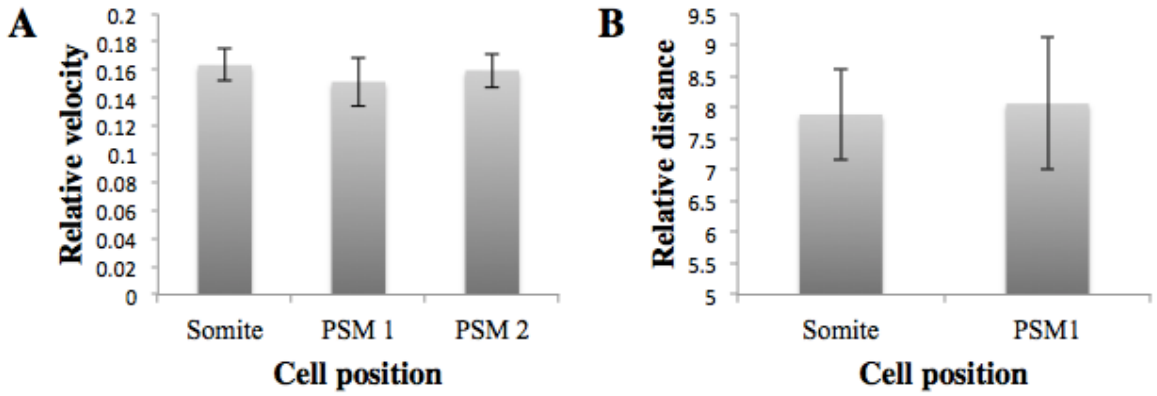

Figure 13. Cell motility activity within somite and PSM region. (A) Relative velocity, (B) Relative distance. Data are represented as means + SE.

Figure 13 showed that both velocity and distance (cell directionality) of somite and PSM cells do not how any significant different. These data indicate that cells in the Erk boundary within PSM undergo minimal movements and maintain spacing among them.

In WT, because they show regular movement of stepwise pattern of Erk, cell in the Erk activity boundary will become the real somite boundary around 2 hours later. But this timing cannot predict in *her1* and *her7* KD. By knocking down two segmentation clock genes, *her1* and *her7*, the dynamic behavior of FGF/Erk activity boundary within PSM showed that both tempo and size of stepwise shift (stepsize) of future somite boundary become irregular.

In addition, cell tracing and length measurement analyses reveal that cell arrangement did not change around the future somite boundary within the PSM, and stepsize of future somite boundary have high correlation with the size of corresponding somites. These results therefore suggest that the stepsize of future somite boundary controls self-organization of cells and size of cell assembly within PSM.

Taken all together, my study shows a dynamic crosstalk between the segmentation clock and signaling gradient. Meeting point between Erk activity boundary and the timing always occurs in the sloping line (wavefront); it suggests that the position of future somite

boundary is determined on the wavefront. In addition, I find that segmentation clock controls the regularity of stepwise pattern of FGF/Erk activity boundary, which will become the somite boundary to make a proper metameric structure of vertebrae. Furthermore, this study provides novel information that spatial information of FGF/Erk activity boundary and its stepwise movement have an important role in self-organization within the PSM to generate somite.

V. Acknowledgements

My sincere gratitude goes to Prof. Yasumasa Bessho and Assoc. Prof. Takaaki Matsui for continuous guidance, support, and invaluable discussions throughout my study.

I wish to express my sincere thanks to Prof. Masashi Kawaichi, Prof. Naoyuki Inagaki, and Assoc, Prof. Noriyaki Sasai, for invaluable discussions and advices as Doctoral supervising committees.

Ass. Prof. Yasukazu Nakahata and Ass. Prof. Norihiro Kitagawa for continuous support, and invaluable discussions.

I am very grateful to Ass. Prof. Ryutaro Akiyama, Dr. Naoyuki Tahara, and Kenny Lischer for invaluable discussions and excellent technical helps and assistance.

To all members of Laboratory of Gene Regulation Research–NAIST, thank you for continuous supports, finest technical helps and assistance, and for very good academic atmosphere.

I would like to thanks to Fisheries Department, Agriculture Faculty, Universitas Gadjah Mada, Hitachi Global Foundation, NAIST Global COE Program and Gene of Regulation Research Laboratory for education opportunity and financial support.

VI. References

Akiyama, R., Masuda, M., Tsuge, S., Bessho, Y., and Matsui, T. (2014). An anterior limit of FGF/Erk signal activity marks the earliest future somite boundary in zebrafish. Development *141,* 1104-1109.

Aulehla, A., Wehrle, C., Brand-Saberi, B., Kemler, R., Gossler, A., Kanzler, B., and Herrmann, B.G. (2003). Wnt3a plays a major role in the segmentation clock controlling somitogenesis. Dev. Cell. *4,* 395-406.

Bessho, Y., Hirata, H., Masamizu, Y., and Kageyama, R. (2003). Periodic repression by the bHLH factor Hes7 is an essential mechanism for the somite segmentation clock. Genes Dev. *17,* 1451-1456.

Bessho, Y., and Kageyama, R. (2003). Oscillations, clocks and segmentation. Curr. Opin. Genet. Dev. *13,* 379-384.

Bessho, Y., Miyoshi, G., Sakata, R., and Kageyama, R. (2001a). Hes7: a bHLH-type repressor gene regulated by Notch and expressed in the presomitic mesoderm. Genes Cells *6,* 175-185.

Bessho, Y., Sakata, R., Komatsu, S., Shiota, K., Yamada, S., and Kageyama, R. (2001b). Dynamic expression and essential functions of Hes7 in somite segmentation. Genes Dev. *15,* 2642-2647.

Brent, A.E., and Tabin, C.J. (2002). Developmental regulation of somite derivatives: muscle, cartilage and tendon. Curr. Opin. Genet. Dev. *12,* 548-557.

Buchberger, A., Bonneick, S., Klein, C., and Arnold, H.H. (2002). Dynamic expression of chicken cMeso2 in segmental plate and somites. Dev. Dyn. *223,* 108-118.

Buchberger, A., Seidl, K., Klein, C., Eberhardt, H., and Arnold, H.H. (1998). cMeso-1, a novel bHLH transcription factor, is involved in somite formation in chicken embryos. Dev. Biol. *199,* 201-215.

Cooke, J., and Zeeman, E.C. (1976). A clock and wavefront model for control of the number of repeated structures during animal morphogenesis. J. Theor. Biol. *58,* 455-476.

Dequeant, M.L., Glynn, E., Gaudenz, K., Wahl, M., Chen, J., Mushegian, A., and Pourquie, O. (2006). A complex oscillating network of signaling genes underlies the mouse segmentation clock. Science *314,* 1595-1598.

Dequeant, M.L., and Pourquie, O. (2008). Segmental patterning of the vertebrate embryonic axis. Nat. Rev. Genet. *9,* 370-382.

Dias, A.S., de Almeida, I., Belmonte, J.M., Glazier, J.A., and Stern, C.D. (2014). Somites without a clock. Science *343,* 791-795.

Dubrulle, J., McGrew, M.J., and Pourquie, O. (2001). FGF signaling controls somite boundary position and regulates segmentation clock control of spatiotemporal Hox gene activation. Cell *106,* 219-232.

Dubrulle, J., and Pourquie, O. (2004). fgf8 mRNA decay establishes a gradient that couples axial elongation to patterning in the vertebrate embryo. Nature *427,* 419-422.

Dunwoodie, S.L., Clements, M., Sparrow, D.B., Sa, X., Conlon, R.A., and Beddington, R.S. (2002). Axial skeletal defects caused by mutation in the spondylocostal dysplasia/pudgy gene Dll3 are associated with disruption of the segmentation clock within the presomitic mesoderm. Development *129,* 1795-1806.

Forsberg, H., Crozet, F., and Brown, N.A. (1998). Waves of mouse Lunatic fringe expression, in four-hour cycles at two-hour intervals, precede somite boundary formation. Curr. Biol. *8,* 1027-1030.

Goldbeter, A., and Pourquie, O. (2008). Modeling the segmentation clock as a network of coupled oscillations in the Notch, Wnt and FGF signaling pathways. J. Theor. Biol. *252,* 574-585.

Henry, C.A., Urban, M.K., Dill, K.K., Merlie, J.P., Page, M.F., Ki el, C.B., and Amacher, S.L. (2002). Two linked hairy/Enhancer of split-related zebrafish genes, her1 and her7, function together to refine alternating somite boundaries. Development *129,* 3693-3704.

Hirata, H., Yoshiura, S., Ohtsuka, T., Bessho, Y., Harada, T., Yoshikawa, K., and Kageyama, R. (2002). Oscillatory expression of the bHLH factor Hes1 regulated by a negative feedback loop. Science *298,* 840-843.

Holley, S.A., Julich, D., Rauch, G.J., Geisler, R., and Nusslein-Volhard, C. (2002). Her1 and the Notch Pathway Function within the Oscillator Mechanism that Regulates Zebrafish Somitogenesis. Development *129,* 1175-1183.

Hubaud, A., and Pourquie, O. (2014). Signalling dynamics in vertebrate segmentation. Nat. Rev. Mol. Cell Biol. *15,* 709-721.

Jiang, Y.J., Aerne, B.L., Smithers, L., Haddon, C., Ish-Horowicz, D., and Lewis, J. (2000). Notch signalling and the synchronization of the somite segmentation clock. Nature *408,* 475-479.

Jouve, C., Palmeirim, I., Henrique, D., Beckers, J., Gossler, A., Ish-Horowicz, D., and Pourquie, O. (2000). Notch signalling is required for cyclic expression of the hairy-like gene HES1 in the presomitic mesoderm. Development *127,* 1421-1429.

Kimmel, C.B., Ballard, W.W., Kimmel, S.R., Ullmann, B., and Schilling, T.F. (1995). Stages of embryonic development of the zebrafish. Dev. Dyn. *203,* 253-310.

Komatsu, N., Aoki, K., Yamada, M., Yukinaga, H., Fujita, Y., Kamioka, Y., and Matsuda, M. (2011). Development of an optimized backbone of FRET biosensors for kinases and GTPases. Mol. Biol. Cell *22,* 4647-4656.

Krol, A.J., Roellig, D., Dequeant, M.L., Tassy, O., Glynn, E., Hattem, G., Mushegian, A., Oates, A.C., and Pourquie, O. (2011). Evolutionary plasticity of segmentation clock networks. Development *138,* 2783-2792.

Leimeister, C., Dale, K., Fischer, A., Klamt, B., Hrabe de Angelis, M., Radtke, F., McGrew, M.J., Pourquie, O., and Gessler, M. (2000). Oscillating expression of c-Hey2 in the presomitic mesoderm suggests that the segmentation clock may use combinatorial signaling through multiple interacting bHLH factors. Dev. Biol. *227,* 91-103.

Mackay, E.W., Apschner, A., and Schulte-Merker, S. (2013). A bone to pick with zebrafish. Bonekey Rep. *2,* 445.

Matsui, T., Raya, A., Kawakami, Y., Callol-Massot, C., Capdevila, J., Rodriguez-Esteban, C., and Izpisua Belmonte, J.C. (2005). Noncanonical Wnt signaling regulates midline convergence of organ primordia during zebrafish development. Genes Dev. *19,* 164-175.

Matsui, T., Thitamadee, S., Murata, T., Kakinuma, H., Nabetani, T., Hirabayashi, Y., Hirate, Y., Okamoto, H., and Bessho, Y. (2011). Canopy1, a positive feedback regulator of FGF signaling, controls progenitor cell clustering during Kupffer's vesicle organogenesis. Proc. Natl. Acad. Sci. U. S. A. *108,* 9881-9886.

McGrew, M.J., Dale, J.K., Fraboulet, S., and Pourquie, O. (1998). The lunatic fringe gene is a target of the molecular clock linked to somite segmentation in avian embryos. Curr. Biol. *8,* 979-982.

Mohammadi, M., McMahon, G., Sun, L., Tang, C., Hirth, P., Yeh, B.K., Hubbard, S.R., and Schlessinger, J. (1997). Structures of the tyrosine kinase domain of fibroblast growth factor receptor in complex with inhibitors. Science *276,* 955-960.

Oates, A.C., and Ho, R.K. (2002). Hairy/E(spl)-related (Her) genes are central components of the segmentation oscillator and display redundancy with the Delta/Notch signaling pathway in the formation of anterior segmental boundaries in the zebrafish. Development *129,* 2929-2946.

Palmeirim, I., Henrique, D., Ish-Horowicz, D., and Pourquie, O. (1997). Avian hairy gene expression identifies a molecular clock linked to vertebrate segmentation and somitogenesis. Cell *91,* 639-648.

Retnoaji, B., Akiyama, R., Matta, T., Bessho, Y., and Matsui, T. (2014). Retinoic acid controls proper head-to-trunk linkage in zebrafish by regulating an anteroposterior somitogenetic rate difference. Development *141,* 158-165.

Roy, M.N., Prince, V.E., and Ho, R.K. (1999). Heat shock produces periodic somitic disturbances in the zebrafish embryo. Mech. Dev. *85,* 27-34.

Saga, Y. (2012). The mechanism of somite formation in mice. Curr. Opin. Genet. Dev. *22,* 331-338.

Saga, Y., Hata, N., Koseki, H., and Taketo, M.M. (1997). Mesp2: a novel mouse gene expressed in the presegmented mesoderm and essential for segmentation initiation. Genes Dev. *11,* 1827-1839.

Sawada, A., Fritz, A., Jiang, Y.J., Yamamoto, A., Yamasu, K., Kuroiwa, A., Saga, Y., and Takeda, H. (2000). Zebrafish Mesp family genes, mesp-a and mesp-b are segmentally expressed in the presomitic mesoderm, and Mesp-b confers the anterior identity to the developing somites. Development *127,* 1691-1702.

Sawada, A., Shinya, M., Jiang, Y.J., Kawakami, A., Kuroiwa, A., and Takeda, H. (2001). Fgf/MAPK signalling is a crucial positional cue in somite boundary formation. Development *128,* 4873-4880.

Sebolt-Leopold, J.S., Dudley, D.T., Herrera, R., Van Becelaere, K., Wiland, A., Gowan, R.C., Tecle, H., Barrett, S.D., Bridges, A., Przybranowski, S., Leopold, W.R., and Saltiel, A.R. (1999). Blockade of the MAP kinase pathway suppresses growth of colon tumors in vivo. Nat. Med. *5,* 810-816.

Stolte, D., Huang, R., and Christ, B. (2002). Spatial and temporal pattern of Fgf-8 expression during chicken development. Anat. Embryol. (Berl) *205,* 1-6.